

**FORMATION OF
VOLATILE NANOPARTICLES
IN MOTOR VEHICLE EXHAUST**

**FINAL REPORT 07-12
SEPTEMBER 2007**

**NEW YORK STATE
ENERGY RESEARCH AND
DEVELOPMENT AUTHORITY**





NYSERDA

The New York State Energy Research and Development Authority (NYSERDA) is a public benefit corporation created in 1975 by the New York State Legislature. NYSERDA's responsibilities include:

- Conducting a multifaceted energy and environmental research and development program to meet New York State's diverse economic needs.
- Administering the **New York Energy SmartSM** program, a Statewide public benefit R&D, energy efficiency, and environmental protection program.
- Making energy more affordable for residential and low-income households.
- Helping industries, schools, hospitals, municipalities, not-for-profits, and the residential sector, including low-income residents, implement energy-efficiency measures.
- Providing objective, credible, and useful energy analysis and planning to guide decisions made by major energy stakeholders in the private and public sectors.
- Managing the Western New York Nuclear Service Center at West Valley, including: (1) overseeing the State's interests and share of costs at the West Valley Demonstration Project, a federal/State radioactive waste clean-up effort, and (2) managing wastes and maintaining facilities at the shut-down State-Licensed Disposal Area.
- Coordinating the State's activities on energy emergencies and nuclear regulatory matters, and monitoring low-level radioactive waste generation and management in the State.
- Financing energy-related projects, reducing costs for ratepayers.

NYSERDA administers the **New York Energy SmartSM** program, which is designed to support certain public benefit programs during the transition to a more competitive electricity market. Some 2,700 projects in 40 programs are funded by a charge on the electricity transmitted and distributed by the State's investor-owned utilities. The **New York Energy SmartSM** program provides energy efficiency services, including those directed at the low-income sector, research and development, and environmental protection activities.

NYSERDA derives its basic research revenues from an assessment on the intrastate sales of New York State's investor-owned electric and gas utilities, and voluntary annual contributions by the New York Power Authority and the Long Island Power Authority. Additional research dollars come from limited corporate funds. Some 400 NYSERDA research projects help the State's businesses and municipalities with their energy and environmental problems. Since 1990, NYSERDA has successfully developed and brought into use more than 170 innovative, energy-efficient, and environmentally beneficial products, processes, and services. These contributions to the State's economic growth and environmental protection are made at a cost of about \$.70 per New York resident per year.

Federally funded, the Energy Efficiency Services program is working with more than 540 businesses, schools, and municipalities to identify existing technologies and equipment to reduce their energy costs.

For more information, contact the Communications unit, NYSERDA, 17 Columbia Circle, Albany, New York 12203-6399; toll-free 1-866-NYSERDA, locally (518) 862-1090, ext. 3250; or on the web at www.nyserderda.org

STATE OF NEW YORK
Eliot Spitzer
Governor

ENERGY RESEARCH AND DEVELOPMENT AUTHORITY
Vincent A. DeIorio, Esq., Chairman
Peter R. Smith, President and Chief Executive Officer

**FORMATION OF VOLATILE NANOPARTICLES
IN MOTOR VEHICLE EXHAUST
FINAL REPORT**

Prepared for the
**NEW YORK STATE
ENERGY RESEARCH AND
DEVELOPMENT AUTHORITY**

Albany, NY
www.nyserda.org

Ellen Burkhard
Project Manager

Prepared by:
UNIVERSITY AT ALBANY
Albany, New York

Fangqun Yu, Ph.D
Project Manager

NOTICE

This report was prepared by University at Albany in the course of performing work contracted for or sponsored by the New York State Energy Research and Development Authority (hereafter “NYSERDA”). The opinions expressed in this report do not necessarily reflect those of NYSERDA or the State of New York, and reference to any specific product, service, process, or method does not constitute an implied or expressed recommendation or endorsement of it. Further, NYSERDA, the State of New York, and the contractors make no warranties or representations, expressed or implied, as to the fitness for particular purpose or merchantability of any product, apparatus, or service, or the usefulness, completeness, or accuracy of any processes, methods, or other information contained, described, disclosed, or referred to in this report. NYSERDA, the State of New York, and the contractors make no representation that the use of any product, apparatus, process, method, or other information will not infringe privately owned rights and will assume no liability for any loss, injury, or damage resulting from, or occurring in connection with, the use of information contained, described, disclosed, or referred to in this report.

PREFACE

The New York State Energy Research and Development Authority (NYSERDA) is pleased to publish “Formation of Volatile Nanoparticles in Motor Vehicle Exhaust.” This project was funded as part of the New York Energy SmartSM Environmental Monitoring, Evaluation and Protection (EMEP) program. More information on the EMEP program may be found on NYSERDA’s website at:

www.nysesda.org/programs/environment/emep/ .

ACKNOWLEDGEMENTS

This research was supported by the New York State Energy Research and Development Authority. The following personnel contributed to this study: Hua Du, Brian Frank, Thomas Lanni, Robert Johnson, Robert Praisner, and Aaron Pulaski.

ABSTRACT

Motor vehicles are known to be a significant source of volatile nanoparticles (NPs) that may cause adverse health effects due to their high number concentration and lung-deposition efficiency. A clear understanding of the mechanisms controlling the formation of these NPs is not only critical to help establish criteria for engine design, operation, after-treatment, fuel and lubricating oil compositional modifications that would effectively reduce NP emissions, but also is important to develop NP emission inventories. Under this project, we have investigated key processes and parameters controlling the formation of volatile NPs in motor vehicle exhaust. It has been proposed previously that ions generated during the combustion via chemiionization reactions (“chemiions”) may be important for NP formation. Experimental measurements of chemiion concentration in the engine exhaust have been made and we find that the concentrations of chemiions in the vehicular exhaust (exiting tailpipe) can reach $\sim 10^7/\text{cm}^3$ during acceleration and are $\sim 10^6/\text{cm}^3$ at idle or running at steady state speed. These concentrations are too low to explain many of the observed NP formation and we conclude that nucleation mechanisms other than chemiion theory must occur in vehicular exhaust. We have developed a kinetic aerosol nucleation model suitable for studying the complex aerosol dynamics in a rapidly diluting engine exhaust and found that binary homogeneous nucleation of sulfuric acid and water can lead to significant formation of NPs in engine exhaust. We have studied the impacts of ambient temperature and relative humidity, fuel sulfur content, sulfur to sulfuric acid conversion efficiency, soot particle concentration, and presence of solid cores on vehicular NP emission indices. Our model simulations show that the low volatile organic species associated with unburned fuel and lubrication oil dominate the growth rate and hence the mass of the nucleation mode particles.

KEY WORDS

Nanoparticles; particulate pollution; engine exhaust; nucleation mechanism; chemiions; health effect

TABLE OF CONTENTS

<u>Section</u>	<u>Page</u>
SUMMARY	S-1
1 INTRODUCTION.....	1-1
2 EXPERIMENTAL MEASUREMENTS AND RESULTS.....	2-1
3 THEORETICAL DEVELOPMENT AND MODELING RESULTS	3-1
4 REFERENCES.....	4-1

FIGURES

<u>Figure</u>	<u>Page</u>
1-1 Schematic illustration of the formation and evolution processes of engine-generated nanoparticles in the atmosphere	1-2
2-1 A schematic showing the experimental design to measure ion concentrations in motor engine exhaust	2-1
2-2 (a) A picture of experimental set-up for chemiion measurements, and (b) measured current (I) as a function of imposed voltage (U) in the exhaust of a K-car (gasoline engine). The K-car used was a 1987 Plymouth Reliant LE 4 Door Wagon with a 4 cylinder, 2.2 liter 97 horsepower gasoline engine.	2-2
2-3 (a) A picture of experimental set-up for chemiion measurements, and (b) measured current (I) as a function of imposed voltage (U) in the exhaust of a diesel generator (diesel engine). The Sentry-Pro 7.5 kW diesel generator is powered by a Kubota model Z482-E, 479 cc, 12.5 horsepower diesel engine.	2-3
2-4 (a) A picture of experimental set-up for chemiion measurements, and (b) time series of imposed voltage and measured current (I) in the exhaust of a Honda gasoline generator..	2-4
2-5 (a) A picture of experimental set-up for chemiion measurements in the exhaust of a 2001 Ford gasoline minivan, and (b) time series of measured currents as the vehicle accelerated from idle to 60 mph and then maintained a speed of 60 mph. Voltage imposed was 500 V	2-5

2-6	The number size distributions (measured with EEPS, averaged over the entire steady state test run) of particles in the exhaust of a 2001 Ford gasoline minivan running at four different speeds. The concentrations are corrected with regard to the dilution	2-6
3-1	Nucleation rates as a function of sulfuric acid vapor concentration (n_a) at four laboratory conditions. The solid lines are the nucleation rates predicted with our kinetic quasi-unary H ₂ SO ₄ -H ₂ O nucleation model (JKQUN). The dot-dashed lines are the nucleation rates predicted by the most recent version of classical binary homogeneous nucleation model (JCBHN) (Vehkamaki et al., 2002)	3-3
3-2	Effect of ambient temperature (T_a) and relative humidity (RH _a) on the concentration of particles larger than 3 nm ($N_{d>3 \text{ nm}}$) at exhaust plume age of 1 s (and the corresponding NP emission index). FSC is set to be 330 ppm, $\epsilon_s = 1\%$, $N_{\text{soot}} = 10^7 \text{ cm}^{-3}$. The shaded rectangle area is the range of on-road emission index (#/kg-fuel) from Kittelson et al. (2004).	3-5
3-3	The dependence of $N_{d>3 \text{ nm}}$ (at $t = 1 \text{ s}$) and NP emission index on fuel sulfur content at two T_a (273 K and 298 K) and RH _a (30% and 80%). $\epsilon_s = 1\%$, $N_{\text{soot}} = 10^7 \text{ cm}^{-3}$	3-5
3-4	The influences of ϵ_s on $N_{d>3 \text{ nm}}$ (at $t=1 \text{ s}$) and NP emission index at three different FSC (330 ppm, 100 ppm, 50 ppm). T_a and RH _a is 283 K and 60%, respectively. $N_{\text{soot}} = 10^7 \text{ cm}^{-3}$	3-6
3-5	The effects of soot particle number concentration on $N_{d>3 \text{ nm}}$ (at $t = 1 \text{ s}$) and NP emission index, at two different FSCs (200 ppm and 330 ppm) and T_a (273 K and 293 K). The ambient relative humidity is 60% and $\epsilon_s = 1\%$	3-7
3-6	Number size distributions of NP formation and evolution on and near the roadway at six selected plume ages under high sulfur condition (FSC=330 ppm). The ambient temperature and relative humidity are assumed to be 278 K and 60 %, respectively. The size-distributions are not corrected with regard to dilution.	3-8
3-7	Simulated volume size distributions of H ₂ SO ₄ , semi- and low volatile organics and soot in the particles at (a) $t=1 \text{ s}$ (a) and (b) $t=10 \text{ s}$ for the case shown in Figure 3.6.....	3-9
3-8	(a) Number size distributions of NPs at four selected plume ages, and (b) volume size distributions for different components at plume age of 1 s for the case with the presence of nanometer-sized solid cores. $T = 298 \text{ K}$, $\text{RH} = 50\%$, $\text{FSC} = 50 \text{ ppm}$, and $\epsilon = 2.5 \%$	3-11

SUMMARY

Engine-generated particles are known to contribute substantially to particulate pollution, especially in urban regions or areas near heavily traveled roads. In addition to the primary soot particles, engine exhaust may contain high concentration of secondary nucleation mode particles (also called volatile ultrafine particles or nanoparticles). There is a growing interest in volatile nanoparticle (NP) emissions from motor vehicles, mainly as a result of suggestions that a decrease in the particle sizes increases its toxicity and indications that reductions in mass emissions of fine particles may increase number emissions of volatile NPs. The volatile NPs, which usually dominate the particle number concentration, may contribute directly to adverse health effects. Recent studies indicate that nanoparticles, after inhaled, can enter the blood circulation and may lead to adverse effect on vital organs such as brain, heart, etc. A firm physical understanding of the processes and parameters controlling formation and growth of volatile NPs in motor vehicle exhaust is critical (1) to design effective control strategies to reduce engine particle number emission; (2) to assess the impact of currently used (or proposed) devices to reduce engine mass emission on number emission; (3) to develop aerosol number emission inventories that are important for assessing the health, chemical, and climatic effects of aerosols. The major objective of this project is to delineate the key processes and parameters controlling the formation of high concentration of volatile NPs or nucleation mode particles observed in motor vehicle exhaust.

It has been proposed in our previous study that ions generated during fuel combustion via chemiionization reactions might play an important role in the formation of volatile NPs (i.e., Chemiion theory). Experimental studies are needed to verify - or rule out - the chemiion theory. Specifically, it is critical to know if the concentration of ions in the exhaust is high enough to explain the observed concentration of volatile NPs. Laboratory experiments have been designed and carried out to obtain chemiion concentrations in engine exhaust. Our measurements indicate that the concentrations of chemiions in the vehicular exhaust (exiting tailpipe) can reach $\sim 10^7/\text{cm}^3$ during acceleration and are $\sim 10^6/\text{cm}^3$ at idle or running at steady state speed—too low to explain many of the observed NP formation (as high as 10^8 - $10^9/\text{cm}^3$, dilution corrected). We conclude that nucleation mechanisms other than chemiion theory must be involved in the formation of volatile particles in vehicular exhaust.

Our finding of the insufficient ions in the engine exhaust to explain the measured NP concentrations prompts us to look into the other possible nucleation mechanism: H_2SO_4 - H_2O binary homogeneous nucleation (BHN). Our analysis indicates that the existing classical BHN model is unsuitable for simulating the particle formation in the rapidly diluting engine exhaust, as its assumption of immediate equilibrium cluster distribution is likely to be invalid. We have devoted significant effort to develop a new kinetic BHN model that simulates the evolution of cluster size spectra explicitly, and thus enables us to clarify confidently the contribution of BHN to the formation of new particles in the engine exhaust diluting in the

real atmosphere. With the new nucleation model, we have comprehensively investigated the conditions for the homogeneous nucleation to become important and the influence of important parameters on NP emission index (EI, in #/kg-fuel). We found that BHN may significantly contribute to the NP formation, especially when the ambient temperature is low and the relative humidity is high. Our simulations show that BHN rate is very sensitive to FSC and sulfur to sulfuric acid conversion efficiency (ϵ_s). For ϵ_s value of 1% and under typical conditions, BHN is significant when FSC $> \sim 200$ ppm, but is negligible when FSC is $< \sim 100$ ppm. NP formation via BHN may still be significant if $\epsilon_s > \sim 4\%$ even after FSC is reduced to below ~ 50 ppm. Our study indicates that the effect of soot scavenging on NP formation via BHN is significant only when soot particle concentration in the raw exhaust is $> \sim 10^7 \text{ cm}^{-3}$. In addition to enhanced sulfur to sulfuric acid conversion efficiency associated with effective exhaust after treatment devices, storage/release effect and non-volatile nanometer-sized cores/particles will also enhance the formation of nanoparticles in the exhaust of the vehicles running on ultra low sulfur fuel. Model simulations have been carried out to study the contribution of low volatile organics to the growth and mass of nucleated mode particles in engine exhaust. The low volatile organic species associated with unburned fuel and lubrication oil appear to dominate the growth rate and hence the mass of the nucleation mode particles. This research highlights the complexity of the tailpipe volatile nanoparticle emissions. Since most of volatile nanoparticles are formed within the first few seconds of exhaust entry into the ambient air and many factors can affect NP formation, proper characterization of volatile NP emissions remains a challenging task.

1 INTRODUCTION

Concerns about the engine nanoparticle (NP) emissions are growing (Kittelson, 1998), mainly as a result of suggestions that a decrease in particle sizes increases its toxicity (e.g., Oberdörste et al., 1995; Seaton et al., 1995; Donaldson et al., 1998; Maynard, 2000) and indications that reductions in mass emissions may increase number emissions of NPs (Bagley et al., 1996). Some studies found that particle number (dominated by NPs) correlated better than fine particle mass with increased symptoms in respiratory effects (e.g., Peters et al., 1997) while others find both particle number and particle mass are associated with mortality (Wichmann et al., 2000). Nemmar et al. (2002) showed that inhaled nanometer carbon particles (5-10 nm) passed rapidly into the systemic circulation, and suggested that this process could account for the well-established, but poorly understood, extrapulmonary effects of nanoparticle pollution. The adverse health effects of engine-generated NPs have also been noted in a number of more recent studies (Wold et al. 2006; Gauderman et al. 2007; Meng et al. 2007; Rundell et al. 2007).

In view of the strong adverse health effects associated with NPs, future standards might be imposed on the number emissions of NPs, and NP emissions from gasoline engines may become a concern as well (Kittelson, 1998). Current mass based emission standards focus only on diesel engines because mass emissions of gasoline engines are much lower. It is important to note that technologies needed to reduce the particle number emissions may be quite different from the ones currently used to reduce the mass emissions. Effective and least costly means of NP emission reduction must be based on a firm physical understanding of the processes and parameters controlling formation and evolution of NPs in vehicle exhaust. Such an understanding is critical to help establish criteria for engine design, operation, after-treatment, and fuel and lubricating oil compositional modifications that would effectively reduce NP emissions. Such an understanding is also important to develop aerosol emission inventories that are important for assessing the health, chemical, and climatic effects of aerosols.

Both measurements and theoretical investigations are needed to understand the processes and parameters controlling formation and evolution of NPs in vehicle exhaust. A database of measurements of NPs from motor vehicles (both in the laboratory and in real atmosphere) is rapidly accumulating (e.g., Abdul-Khalek et al., 1999; Shi and Harrison, 1999; Kittelson et al., 2003, 2004, 2006a,b; Tobias et al., 2001; Maricq et al., 2002a,b; Sakurai et al., 2003; Jung et al., 2005; Kuhn et al. 2005a,b; Zhu et al., 2002a, b, 2004, 2006; Rönkkö et al., 2006; Biswas et al. 2007). These observations provide useful information on NP properties (number concentrations, sizes, and compositions) and various parameters affecting these properties. The parameters that have been observed to affect the NP properties include: fuel sulfur content, dilution conditions (dilution ratio, temperature and relative humidity of diluting air), soot particle concentrations, sampling line residence time, vehicular speed, and engine operation conditions (loading, cold or hot starting, acceleration, etc.).

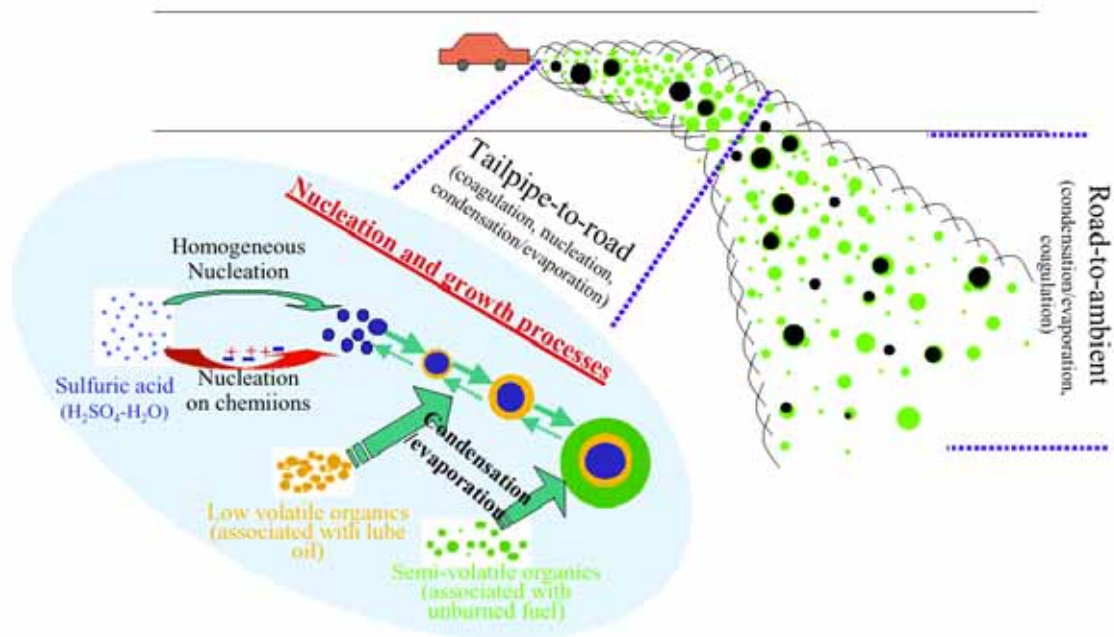


Figure 1-1. Schematic illustration of the formation and evolution processes of engine-generated nanoparticles in the atmosphere.

Figure 1 shows schematically the major processes involved in the formation and evolution of NPs in the engine exhaust diluting in the atmosphere. The engine exhaust experiences two distinct dilution stages: (1) tailpipe-to-road and (2) road-to-ambient. In the first stage, tailpipe-to-road dilution, the exhaust is diluted by strong turbulence generated by moving traffic, and dilution ratio reaches around 1000 in 1-5 s. In the second stage, road-to-ambient dilution, the exhaust is further diluted by a factor of around 10 in 200-600 s by atmospheric turbulence induced by wind and atmospheric instability (Zhang et al., 2004).

Under typical dilution conditions, the exhaust approaches the temperature and relative humidity of ambient air at exhaust age (t) of less than 0.1 s. When certain precursor vapors (in our case $H_2SO_4-H_2O$) are supersaturated as the exhaust cools down, nucleation happens rapidly and our preliminary simulations indicate that nucleation is usually negligible at $t > \sim 0.1$ s. The fresh nucleated particles continue to grow by taking up low volatile precursors (including organic compounds) and some of them are lost due to coagulation. Since different organic compounds have different saturation vapor pressures and Kelvin effects, it is only after the nucleated particles grow to a certain size that certain organic compounds begin to condense on these particles. The general mechanism of engine NP formation, involving binary nucleation of $H_2SO_4-H_2O$ followed by condensation growth of organic compounds, has been reported in the literature

(Baumgard and Johnson, 1996; Shi and Harrison, 1999; Abdul-Khalek et al., 2000; Tobias et al., 2001). When the exhaust is dispersed further, some organic precursors become under-saturated with respect to small particles due to large Kelvin effect, and as a result, small particles may experience evaporation shrink while some relatively large particles may continue to grow (Robinson et al., 2007). Newly formed particles (and precursor vapors) are continuously scavenged by pre-existing particles.

Compared to the rapidly accumulating measurements of NPs from motor vehicles, the fundamental studies that quantitatively explain these measurements are lacking, and a clear understanding of how particles form and evolve in engine exhaust and how different parameters affect the particle properties remains to be achieved. The main objective of this project is to delineate the key processes and parameters controlling the formation and evolution of NPs in vehicle exhaust, through laboratory measurements, theoretical and model development, numerical modeling, and data analyses.

2 EXPERIMENTAL MEASUREMENTS AND RESULTS

In view of the difficulty of classical binary nucleation theory in explaining some key properties (number concentrations and their dependence on fuel sulfur contents) of nanoparticles in engine exhaust observed in the laboratory, Yu (2001) proposed that chemiions generated during fuel combustion might play an important role in the formation of these nanoparticles (i.e., Chemiion theory). Yu (2001) showed that the total number of nanoparticles formed in motor vehicle exhaust is very sensitive to chemiion concentrations. Experimental studies are needed to verify - or rule out - the chemiion theory. Specifically, it is critical to know if the concentration of ions in the exhaust is high enough to explain the observed concentration of nucleated nanoparticles.

Laboratory experiments to measure chemiion concentrations in the exhaust of different engines were designed and carried out at the Automotive Emissions Laboratory in the Bureau of Mobile Sources and Technology Development of the Division of Air Resources of the NYS Dept. of Environmental Conservation. Figure 2-1 shows schematically the experimental design used to measure ion concentrations in motor vehicles exhaust (Yu et al., 2004). A conductive pipe is connected to the engine pipe with proper insulation. An adjustable electrostatic potential (U) is imposed on the exhaust passing through the conductive pipe via a rod placed at the center of the pipe. A is the electrometer and V is the voltage source. Ion concentration can be estimated based on the current (I) measured by the electrometer and the exhaust flow rate.

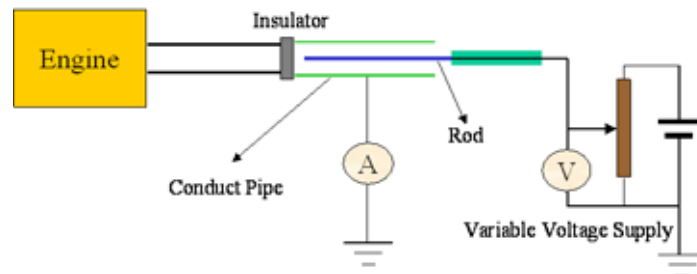


Figure 2-1. A schematic showing the experimental design to measure ion concentrations in motor vehicles exhaust. (from Yu et al., 2004)

As a result of electrostatic forces, ions in the exhaust are collected by the conductive pipe and rod. The relationship between the concentration of ions in the exhaust and the current (I) measured by the electrometer is straightforward. The current (I) measured by the electrometer is equal to the production of elementary charge and the number of ions collected by the probe per unit time, which is equal to the concentration of ions (already collected) multiplied by the exhaust flow rate. From the current (I) measured by electrometer, the average concentration of ions (of one sign) in the exhaust that have already been

collected can be estimated as

$$\overline{[ion]} = \frac{I/e}{v} \quad (1)$$

where $e=1.6 \times 10^{-19}$ C is the elementary charge. v (liters per minute) is the exhaust flow rate, which can be estimated from fuel consumption rate and air fuel ratio. Generally speaking, smaller ions have higher mobility and need lower imposed voltage (U) to be collected by the conductive pipe. I is expected to increase with increasing U as more ions are collected at higher U . If the voltage is high enough, all ions in the exhaust can be collected and then I will not increase when U increases further.

Figures 2.2-5 are experimental set up pictures and results of a series of measurements made at AEL Hemlock St. Lab. We measured the concentrations of ions in the exhaust of diesel and gasoline engines (or generators) when different voltages were imposed. In some cases, TSI Scanning Mobility Particle Sizer (SMPS) spectrometer and Engine Exhaust Particulate Spectrometer (EEPS) were also used to measured particle size distributions.

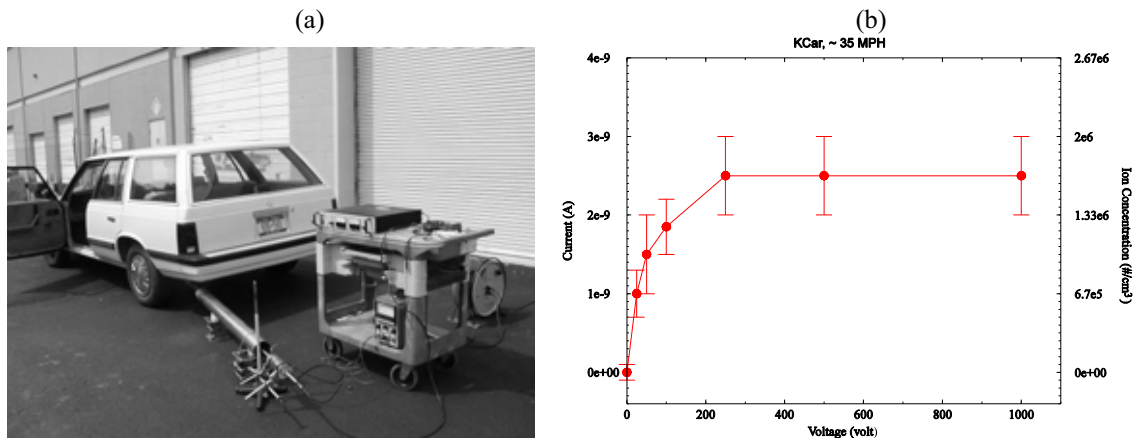


Figure 2.2. (a) A picture of experimental set-up for chemion measurements, and (b) measured current (I) as a function of imposed voltage (U) in the exhaust of a K-car (gasoline engine). The K-car used was a 1987 Plymouth Reliant LE 4 Door Wagon with a 4 cylinder, 2.2 liter 97 horsepower gasoline engine. (from Yu et al., 2004)

Figure 2.2 shows the experimental set-up and observed values for chemion measurements in the exhaust of a K-car (gasoline engine). For the K-car, the conductive pipe was connected to the end of the tailpipe and the residence time of the exhaust inside the tailpipe or connection pipe before entering the conductive pipe is ~ 0.7 s. The residence time is estimated from the exhaust flow rate. The imposed voltage U was adjusted manually and the corresponding current I was recorded. Since the engine did not run in an absolute stable condition and the flow inside the pipe was turbulent, the measured I values fluctuated at a given U . The error bars shown in the figure indicate the range of these fluctuations.

Figure 2.2(b) gives the changes in measured I as U increases from 0 V to 1000 V in the exhaust of the K-car, and the corresponding total ion concentrations (positive ions + negative ions) estimated using equation (1) are also given. The K-car was running at ~ 35 mph and the exhaust flow rate was ~ 560 liter per minute. When no voltage was imposed ($U = 0$ V), the values of I fluctuated between -1.0×10^{-10} A and $+1.0 \times 10^{-10}$ A, suggesting that both positive and negative ions diffuse into the inner wall of the conductive tube. As U increases, the observed current increases, and when $U=250$ V the measured current I reaches a maximum value of around $2.5 \pm 0.5 \times 10^{-9}$ A (corresponding to a total ion concentration of $\sim 3.3 \pm 0.66 \times 10^6$ cm^{-3}). When $U > 250$ V, I does not change as U increases, which suggests that all ions in the exhaust have been collected. Based on equation (2), all ions in the exhaust with mobility less than ~ 0.2 $\text{cm}^2 \text{v}^{-1} \text{s}^{-1}$ should have been collected at $U=250$ V. As discussed earlier, in general ions with larger sizes (lower mobility) are collected at higher voltage. The continuous increase in I as U increases when $U < 250$ V suggests that the size or mass of ions in the gasoline engine exhaust has a wide range. Since the corresponding diameter of ions with mobility of 0.2 $\text{cm}^2 \text{v}^{-1} \text{s}^{-1}$ is ~ 3 nm, we can conclude that most of the ions in the exhaust of the K-car are smaller than ~ 3 nm.

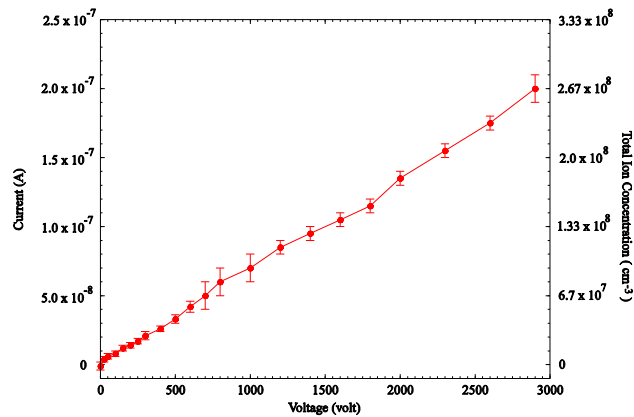
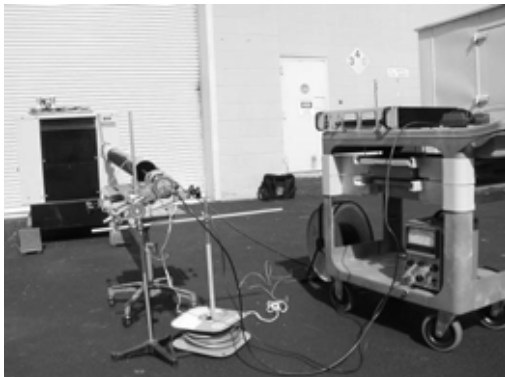


Figure 2.3. (a) A picture of experimental set-up for chemiion measurements, and (b) measured current (I) as a function of imposed voltage (U) in the exhaust of a diesel generator (diesel engine). The Sentry-Pro 7.5 kW diesel generator is powered by a Kubota model Z482-E, 479 cc, 12.5 horsepower diesel engine. (from Yu et al., 2004)

Figure 2.3 shows the experimental set-up and observed values for chemiion measurements in the exhaust of a diesel generator. The diesel generator was operating at 50% load. Figure 2.3(b) presents the measured I - U curve and the corresponding total ion concentrations. At $U = 0$ V, the values of I fluctuate between -4.0×10^{-9} A and $+2.0 \times 10^{-9}$ A with an average value of -1.0×10^{-9} A. Note that the magnitude of the fluctuation at $U = 0$ V in the diesel exhaust is more than one order of magnitude larger than that in the K-car exhaust, which suggests a much higher concentration of small ions in the diesel exhaust at the measurement point. The average negative current at $U=0$ V indicates that the mean mobility of negative ions is higher than that

of positive ions. When a positive voltage is imposed, a positive current appears and the current measured increases almost linearly with imposed voltage (0V - 2900V). The observed currents in the exhaust of the diesel generator are $\sim 1.7 \pm 0.2 \times 10^{-8}$ A at $U = 250$ V and $\sim 2.0 \pm 0.1 \times 10^{-7}$ A at $U = 2900$ V, which correspond to a total ion concentration of $2.26 \pm 0.26 \times 10^7$ cm⁻³ and $2.67 \pm 0.13 \times 10^8$ cm⁻³ respectively (based on exhaust flow rate of 560 liter per minute).

The mobility of ions completely collected is estimated to be ≤ 0.2 cm² v⁻¹ s⁻¹ (corresponding to a diameter of ≤ 3 nm) at $U = 250$ V and ≤ 0.019 cm² v⁻¹ s⁻¹ (corresponding to a diameter of ≤ 10 nm) at $U = 2900$ V.

While all ions/charged particles ≤ 10 nm are expected to be collected at U of 2900 V, some particles > 10 nm may also have been collected if they were in the exhaust close to the wall. The diesel engine used in this study has a very high emission index of soot particles (on the order of 10^8 /cm³), and when a high voltage was imposed, some charged soot particles were collected. The increase in the measured current as U increases when $U > 250$ V is likely due to the collection of these charged soot particles. In contrast to the diesel engine, the soot emission index of the gasoline engine (K-car) is much lower (the concentration of soot particles in the exhaust is on the order of 10^4 cm⁻³), which may explain why no visible change in the current is observed even when the voltage imposed on the K-car exhaust increased from 250 V to 3000 V.

When the imposed voltage is less than 250 V, the measured current (and hence the concentration of collected ions) in the diesel exhaust is about one order of magnitude higher than that in the K-car exhaust. This difference is likely due to the much shorter residence time (~ 0.15 s) of exhaust inside the pipe connecting the conductive pipe and the diesel engine. The residence time of exhaust inside the K-car tailpipe is ~ 0.7 s. The concentration of small ions in the exhaust drops significantly in the first 0.5 s inside the tailpipe or connecting pipe as a result of ion-ion recombination, soot scavenging, and wall loss.

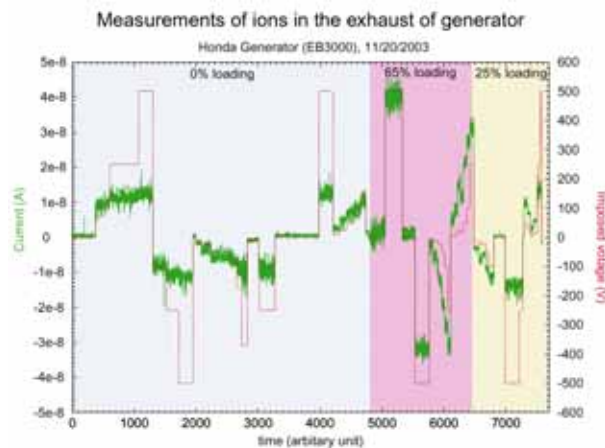


Figure 2.4. (a) A picture of experimental set-up for chemion measurements, and (b) time series of imposed voltage and measured current (I) in the exhaust of a Honda gasoline generator.

Figure 2.4 presents another set of measurements made in the exhaust of a Honda gasoline generator. During this study, the currents were measured by a digital pico-ammeter when different voltages were imposed to the exhaust. The Honda generator was running at three different loadings (0%, 65%, and 25%). The measured values of currents (in A) can be converted to the ion concentrations (cm^{-3}) by multiplying $3.1 \times 10^{15} \text{ A cm}^{-3}$ (0% loading), $2.3 \times 10^{15} \text{ A cm}^{-3}$ (25% loading), $1.4 \times 10^{15} \text{ A cm}^{-3}$ (65% loading). Measured ion concentrations increase with the voltage but reach a saturation value when voltage is above $\sim 250 \text{ V}$. The maximum ion concentrations change slightly with loading and are $\sim 5.6 \times 10^7 \text{ cm}^{-3}$ for 65% loading.

Chemiion experiment carried out in the exhaust of a 2001 Ford gasoline Minivan was shown in Figure 2.5. Our measurements indicate that high concentrations of chemiions were in the exhaust only when the vehicle was on acceleration. As the vehicle was accelerated from idle to 60 mph, the measured currents increased by a factor of 30 (from 10^{-9} A to $3 \times 10^{-8} \text{ A}$) and the corresponding chemiion concentrations increased from $\sim 10^6 / \text{cm}^3$ to $\sim 10^7 / \text{cm}^3$ (note that the exhaust flow rates are different for two speeds). When the vehicle maintains a steady-state speed of around 60 mph, the observed currents dropped to $\sim 10^{-9} \text{ A}$ (chemiion concentrations $< 10^6 / \text{cm}^3$). Similar measurements were also carried out in the exhaust of a 1999 Dodge diesel pick-up. The measured chemiion concentrations are generally similar to previous observations that show that high concentrations of chemiions were observed only during acceleration.

We have also measured the size distributions of particles with SMPS and EEPS in diluted exhaust as the undiluted exhaust is passed through a variable electric field. If the chemiion theory is correct, we should see a change in the number of nanoparticles formed as the current shown via microammeter changes due to varying voltage. Unfortunately, we didn't see obvious nucleation mode particles in the SMPS measured size distributions. There are three possible explanations: (1) no nucleation mode particles were formed under the conditions; (2) nucleation happened but the SMPS were not able to detect these particles due to the detection limit; (3) wall loss in the sample line inhibited the nucleation.

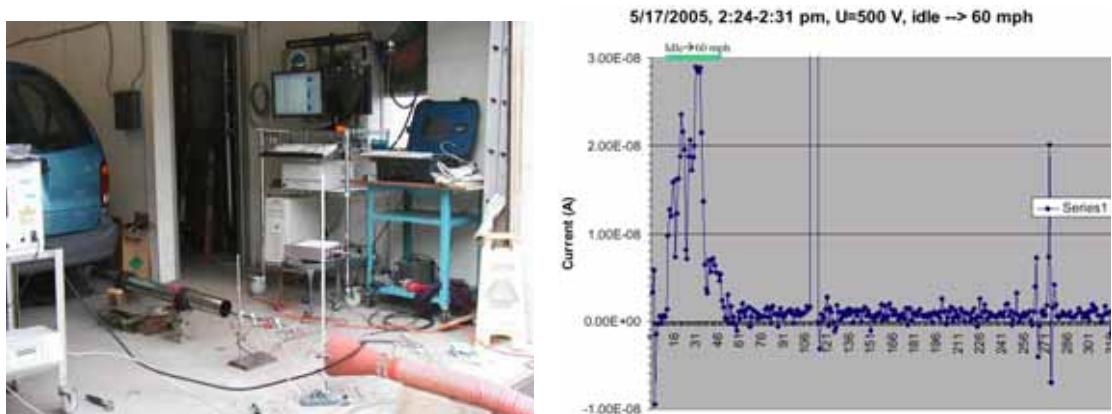


Figure 2.5. (a) A picture of experimental set-up for chemiion measurements in the exhaust of a 2001 Ford gasoline minivan, and (b) time series of measured currents as the vehicle accelerated from idle to 60 mph and then maintained a speed of 60 mph. Voltage imposed was 500 V.

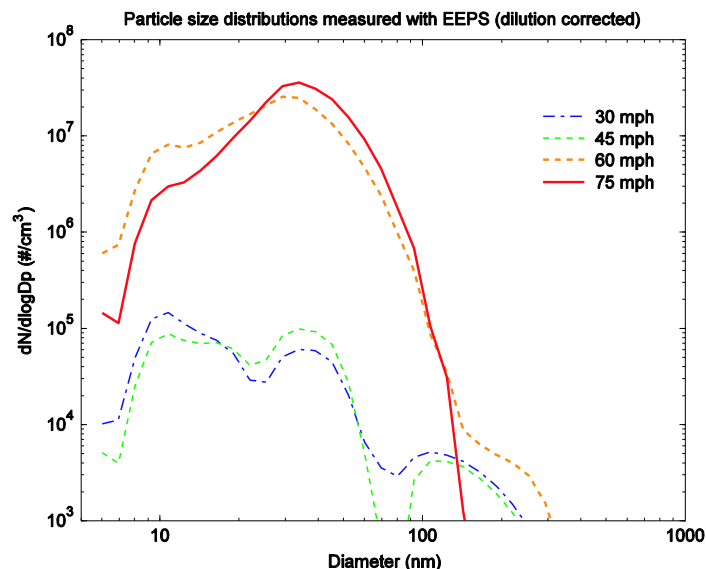


Figure 2.6. The number size distributions (measured with EEPS, averaged over the entire steady state test run) of particles in the exhaust of a 2001 Ford gasoline minivan running at four different speeds. The concentrations are corrected with regard to the dilution.

Figure 2.6 shows the measured number size distributions of particles in the exhaust of a 2001 Ford gasoline minivan running at four different speeds. Our measurements indicate that the gasoline minivan emits very high concentration of nanoparticles when running at high speed ($> \sim 60$ mph). The concentrations (with dilution correction) can reach above $10^7/\text{cm}^3$, which are in the same order of magnitude as those emitted from typical diesel vehicles. The median sizes of these nanoparticles are around 30 - 40 nm. The imposed voltages have no obvious impact on the measured concentrations of these nanoparticles. Currently we don't know how these particles were formed or their compositions, but we expect them to be soot particles. Further research is clearly needed to characterize the nanoparticle emission from gasoline vehicles running at different speeds or operating under different conditions.

In summary, our laboratory experiments indicate that, under typical operation conditions, the concentrations of chemiions in the exhaust of generators are in the range of $10^6 - 10^8/\text{cm}^3$ and are generally below $10^7/\text{cm}^3$ in the exhaust of diesel and gasoline vehicles. Our measurements indicate that the concentrations of chemiions in the vehicular exhaust (exiting tailpipe) can reach $\sim 10^7/\text{cm}^3$ during acceleration and are $\sim 10^6/\text{cm}^3$ at idle or running at steady state speed. It appears that the loss of ions in the tailpipe is significant. While nucleation on ions is known to have advantage over homogenous nucleation, our measurements suggest that the chemiion concentrations in the exhaust are too low to explain many of the observed nanoparticle formations (as high as 10^8 - $10^9/\text{cm}^3$, dilution corrected) and thus nucleation mechanisms other than chemiion theory are likely to be involved in the formation of volatile particles in vehicular exhaust.

3 THEORETICAL DEVELOPMENT AND MODELING RESULTS

3.1. BACKGROUND

The major objective of this project is to delineate the key processes and parameters controlling the formation of high concentration of volatile nanoparticles (NPs) or nucleation mode particles observed in motor vehicle exhaust. Our measurements presented in the previous section show that the chemical concentrations in the exhaust are insufficient to explain many of the observed NP formations. This finding prompts us to look into the other possible nucleation mechanism -- binary homogeneous nucleation (BHN). Earlier studies (Shi and Harrison, 1999; Yu, 2001) have shown that the BHN theory is unable to explain the particle nucleation in the laboratory dilution chamber. Our investigation reveals that, while it is true that BHN theory is unable to explain the particle nucleation observed in the laboratory, BHN may contribute to particle formation in the engine exhaust diluting in the real atmosphere. Our further investigations indicate that the existing **classical** BHN model is unsuitable for simulating the particle formation in the rapidly diluting engine exhaust, as its assumption of immediate equilibrium cluster distribution is likely to be invalid.

We have devoted significant effort to develop a new kinetic binary homogeneous nucleation model (Yu, 2005, 2006). The kinetic nucleation model simulates the evolution of cluster size spectra explicitly, which are necessary when the ambient conditions change rapidly, and thus enables us to simulate with confidence the contribution of $\text{H}_2\text{SO}_4\text{-H}_2\text{O}$ homogeneous nucleation to the formation of new particles in the engine exhaust diluting in the real atmosphere (Du and Yu, 2006). By carrying out extensive sensitivity studies, we seek to understand under what conditions the homogeneous nucleation may become important, and the influence of key parameters on NP emission index (EI, in #/kg-fuel). The key parameters considered in our study include ambient temperature (T_a) and relative humidity (RH_a), fuel sulfur content (FSC), sulfur to sulfuric acid conversion efficiency (ϵ_s , fraction of sulfur in the fuel converted to sulfuric acid), and the number concentration of soot particles in the undiluted exhaust (N_{soot}) (Du and Yu, 2006).

3.2 DEVELOPMENT OF KINETIC NUCLEATION MODEL SUITABLE FOR STUDYING VEHICULAR NP FORMATION

Only sulfuric acid is likely to become supersaturated enough for homogeneous nucleation during diluting vehicular exhaust (Tobias et al., 2001); and various versions of the classical $\text{H}_2\text{SO}_4\text{-H}_2\text{O}$ BHN theory have been applied to study the new particle formation in diluting engine exhaust (Baumgard et al., 1996; Shi and Harrison, 1999; Kim et al., 2002; Zhang and Wexler, 2004). However, there exists a limitation in using classical BHN theory to calculate the particle formation rates in vehicular exhaust. The classical BHN theory assumes that steady-state equilibrium distribution of critical clusters is achieved instantaneously at given H_2SO_4 concentration ($[\text{H}_2\text{SO}_4]$), temperature (T), and relative humidity (RH). The classical BHN

model can not keep track of the cluster distributions in the rapidly diluting engine exhaust due to the dramatic changes in T , RH , and $[H_2SO_4]$ (and resulting size of critical clusters) when fresh engine exhaust mixes with ambient air. The cluster distributions in the rapidly diluting engine exhaust are likely to change quickly and the classical BHN model cannot keep track of these changes properly. Yu (2005, 2006) showed that the BHN of H_2SO_4 - H_2O can be treated as quasi-unary nucleation (QUN) of H_2SO_4 in equilibrium with H_2O vapor, and developed a kinetic H_2SO_4 - H_2O nucleation model. This kinetic model can keep track of the clusters of all sizes in the diluting exhaust experiencing rapid changes in T , RH , and $[H_2SO_4]$, and thus is a more robust method to study engine-generated NPs.

The key assumptions of the kinetic H_2SO_4 - H_2O QUN model (Yu, 2005) include: (1) At given temperature and relative humidity, the sulfuric acid clusters of various sizes are in equilibrium with water, and their average compositions (i.e., number of H_2O molecules i_b in a cluster containing i_a H_2SO_4 molecules) can be approximated using the most stable compositions. (2) The binary H_2SO_4 - H_2O nucleation is controlled by the growth/shrink of $(H_2SO_4)_{i_a}(H_2O)_{i_b}$ clusters (“ i_a -mers”) through the uptake/evaporation of H_2SO_4 molecules. The QUN model effectively decouples the two-dimension nucleation problem into a one-dimension problem that allows obtaining the explicit time-dependent picture of the evolution of pre-nucleation clusters in the nucleating vapors.

The equilibrium (or average) number of H_2O molecules in the i_a -mer (i.e., $i_b(i_a)$) is a function of T and RH only. $i_b(i_a)$ is determined by locating the minimum point of the change in the Gibbs free energy $\Delta G(i_a, i_b)$ in i_b direction (Yu, 2005). When the compositions of clusters $i_b(i_a)$ are known, other cluster properties (radius r_{i_a} , mass m_{i_a} , bulk density, surface tension, etc.) can be decided accordingly. The time-dependent evolution of cluster size distributions can be obtained by solving the following set of differential equations:

$$\frac{dn_{i_a}}{dt} = \beta_{i_a-1}n_{i_a-1} - \gamma_{i_a}n_{i_a} - \beta_{i_a}n_{i_a} + \gamma_{i_a+1}n_{i_a+1} - n_{i_a} \sqrt{\frac{k_B T}{2\pi m_{i_a}}} S, \quad i_a \geq 2 \quad (2)$$

$$\frac{dn_1}{dt} = P - \sum_{i_a=1}^{\infty} \beta_{i_a} n_{i_a} + 2\gamma_2 n_2 + \sum_{i_a=3}^{\infty} \gamma_{i_a} n_{i_a} - n_1 \sqrt{\frac{k_B T}{2\pi m_1}} S \quad (3)$$

where n_{i_a} is the number concentration of clusters containing i_a H_2SO_4 molecules (and $i_b(i_a)$ H_2O molecules); P is the production rate of H_2SO_4 molecules; S is the characteristic surface area of the pre-existing particles; β_{i_a} is the forward (or growth) rate of i_a -mers; and γ_{i_a} is the reverse (or evaporation) rate of H_2SO_4 molecules from i_a -mers. The detailed description of methods used to calculate β_{i_a} and γ_{i_a} have been presented in Yu (2006). The coagulation among clusters is not shown in equation (2) but is considered in our simulations presented in this report.

The kinetic QUN (KQUN) model does not have two well-recognized problems associated with the classical BHN (CBHN) theory (violation of the mass action law and mismatch of the cluster distribution for monomers) and is appropriate for the situations where the assumption of steady state equilibrium cluster distribution is invalid (as in the case of particle formation in engine exhaust). The model uses the most recently available thermodynamic data. We have assessed the performance of our KQUN model by comparing it carefully with the most recent version of classical BHN model (Vehkamaki et al., 2002) as well as experimental data. Figure 3.1 shows that KQUN model gives a much better agreement with experimental data.

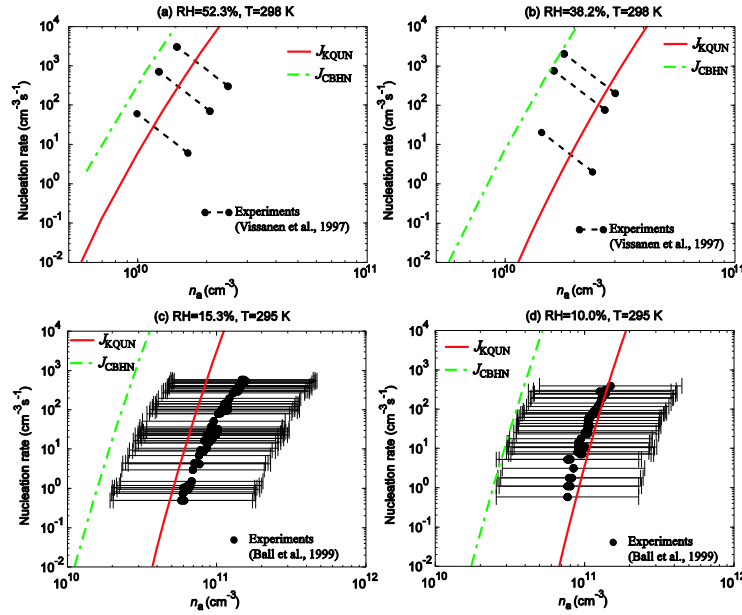


Figure 3.1. Nucleation rates as a function of sulfuric acid vapor concentration (n_a) at four laboratory conditions. The solid lines are the nucleation rates predicted with our kinetic quasi-unary H₂SO₄-H₂O nucleation model (J_{KQUN}). The dot-dashed lines are the nucleation rates predicted by the most recent version of classical binary homogeneous nucleation model (J_{CBHN}) (Vehkamaki et al., 2002). (modified from Yu, 2005)

3.3 DILUTION OF EXHAUST PLUME IN THE ATMOSPHERE

Based on different dominant aerosol microphysical processes taking place inside the plume, the plume evolution can be divided into three distinctive stages. In our study, plume age (t) is defined as the time elapsed after exhaust is emitted out of tailpipe. Stage 1 starts from 0 s to ~1 s of plume age where the hot vehicular exhaust experiences rapid dilution due to strong turbulence in the near field of tailpipe. Nucleation is the key microphysical process in this stage. Studies showed that typical dilution ratios at this stage are ~ 600 – 4400 (Kittelson et al. 1988; Shi et al. 2002). Dilution ratio as function of plume age used in this study was obtained using the nonlinear regression of experimental data of Kittelson et al. (1988).

The equation for the dilution ratio is in the form of $DR = 1 + 700 \times t^{1.413}$ ($t \leq s$). It should be noted that the initial mixing of the exhaust into the air may be much more complex than this simple dilution ratio parameterization. Since nucleation is sensitive to the dilution ratios, the radial heterogeneity of the exhaust plume will have some effect on the particle formation. The actual effect remains to be investigated. The sensitivity studies presented in this report can be used to estimate such effect. The results presented below represent average values.

Stage 2 starts from 1 s of plume age to t_1 (when exhaust is on the roadside). At this stage, low volatile organics still condense onto the nucleated particles, and semi-volatile organics may begin to evaporate due to the dilution (Sakurai et al. 2003). The real dilution that a single on-road vehicle plume may experience is a very complex problem, which depends on vehicle-generated turbulence and mixing with other plumes. Currently no established dispersion model is available to simulate this process and predict the on-road dilution profile for a single plume. In this study, the dilution profile in the second stage was estimated based on the ratio of CO_2 concentration in raw exhaust before dilution to the observed on-road ones. Typically the dilution ratio during stage 2 ($t_1 \sim 5$ s) is around 5 ~ 10, depending on traffic density, wind speed and atmospheric stability. The third stage starts from roadside to any downwind location perpendicular to the roadway. The aerosol processing here involves dilution and organic evaporation. The dilution profile in this stage can be determined from CO measurements and is assumed to be 10 at 100 meters away from the roadside (Zhu et al. 2002a) in this study.

3.4. IMPACTS OF KEY PARAMETERS ON THE FORMATION OF NANOPARTICLES IN VEHICULAR EXHAUST

3.4.1. Ambient Temperature (T_a) and Relative Humidity (RH_a)

Figure 3.2 illustrates $N_{d>3nm}$ as a function of T_a at four RH_a at plume age of 1 s. The corresponding EIs are indicated as well. It shows that NP formation in vehicular exhaust via BHN is significant under a wide range of T_a and RH_a values. Lower T_a and higher RH_a enhance the NP formation. The effect of RH_a on $N_{d>3nm}$ is more significant under high T_a conditions. Under favorable conditions, $N_{d>3nm}$ at plume age of 1s can reach 10^6 cm^{-3} , which corresponds to an EI of $\sim 10^{16} \text{ \#/kg-fuel}$. Kittelson et al. (2004) showed that on-road NP EIs on two Minnesota freeways are in the range of $\sim 2.2 - 11 \times 10^{15} \text{ \#/kg-fuel}$ for a gasoline-dominated vehicle fleet in wintertime conditions with T_a of 274-286 K, RH_a of 40% - 60% and FSC of ~ 330 ppm. On-road NP EIs of around $8.3 \times 10^{15} \text{ \#/kg-fuel}$ have been reported for Helsinki metropolitan area, Finland (Yli-Tuomi et al., 2005). Our simulations indicate that BHN may explain these observed high vehicular NP EIs.

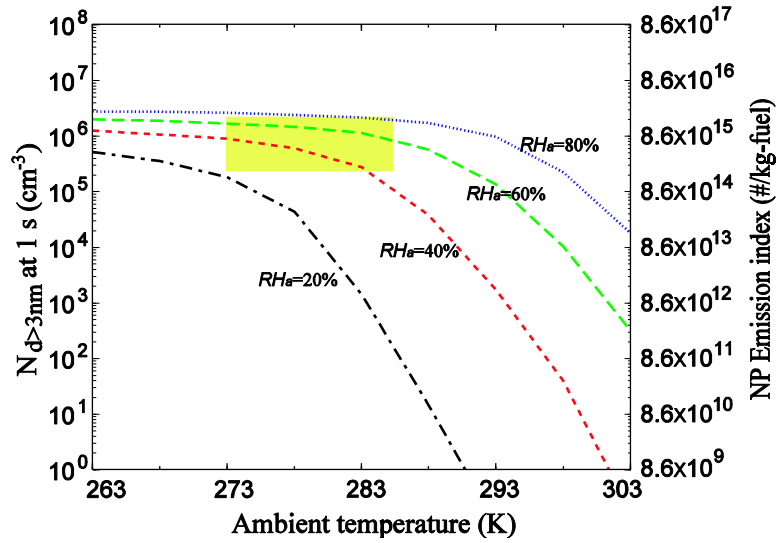


Figure 3.2. Effect of ambient temperature (T_a) and relative humidity (RH_a) on the concentration of particles larger than 3 nm ($N_{d>3 \text{ nm}}$) at exhaust plume age of 1 s (and the corresponding NP emission index). FSC is set to be 330 ppm, $\epsilon_s = 1\%$, $N_{\text{soot}} = 10^7 \text{ cm}^{-3}$. The shaded rectangle area is the range of on-road emission index (#/kg-fuel) from Kittelson et al. (2004).

3.4.2. Fuel Sulfur Content

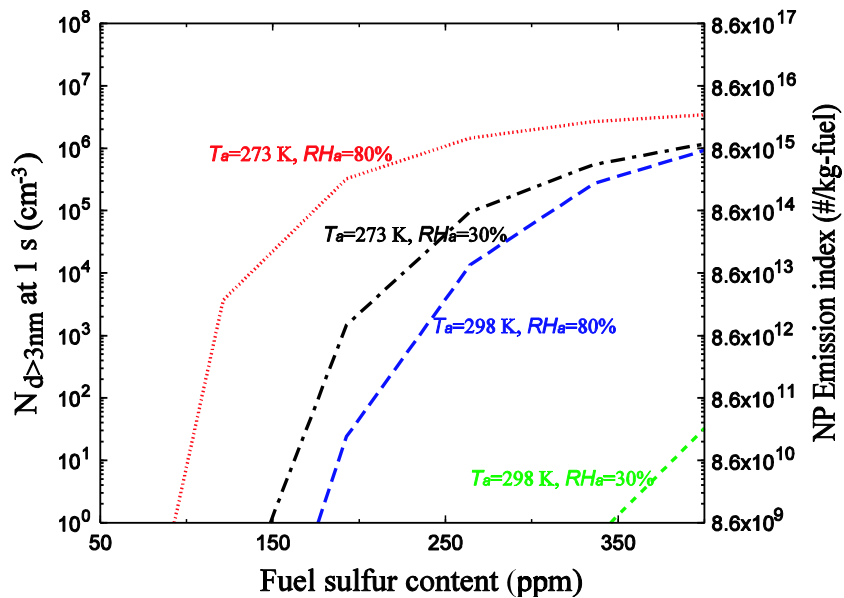


Figure 3.3. Dependence of $N_{d>3 \text{ nm}}$ (at $t = 1 \text{ s}$) and NP emission index on fuel sulfur content at two T_a (273 K and 298 K) and RH_a (30% and 80%). $\epsilon_s = 1\%$, $N_{\text{soot}} = 10^7 \text{ cm}^{-3}$.

Figure 3.3 shows $N_{d>3\text{ nm}}$ at plume age of 1 s as a function of FSC under four different ambient conditions, with a fixed values of ϵ_s (1.0%). Our kinetic model predicts strong sensitivity of $\text{H}_2\text{SO}_4\text{-H}_2\text{O}$ BHN rates to FSC. For example at $T_a = 298\text{K}$ and $\text{RH}_a = 80\%$, the nucleation rates decrease by four orders of magnitude as FSC decreases from 400 to 200 ppm. When $\text{FSC} < 100$ ppm, $\text{H}_2\text{SO}_4\text{-H}_2\text{O}$ BHN is very small in all typical ambient conditions. This indicates that in states such as California, in which fuel with $\text{FSC} < \sim 30$ ppm is used, or in the future when fuel with ultra-low-sulfur content ($\text{FSC} < 15$ ppm) is used, the contribution of binary $\text{H}_2\text{SO}_4\text{-H}_2\text{O}$ homogenous nucleation to new NP formation may become negligible if ϵ_s does not change. The observations of NP formation in the exhaust of engines running on ultra-low sulfur fuel ($\text{FSC} < \sim 15$ ppm) may indicate the involvement of other species, such as ions, organics, metal, or ammonia. However, as we will show below, BHN may still be significant for fuel with ultra low sulfur if ϵ_s is much larger than 1%.

3.4.3. Sulfur to Sulfuric Acid Conversion Efficiency

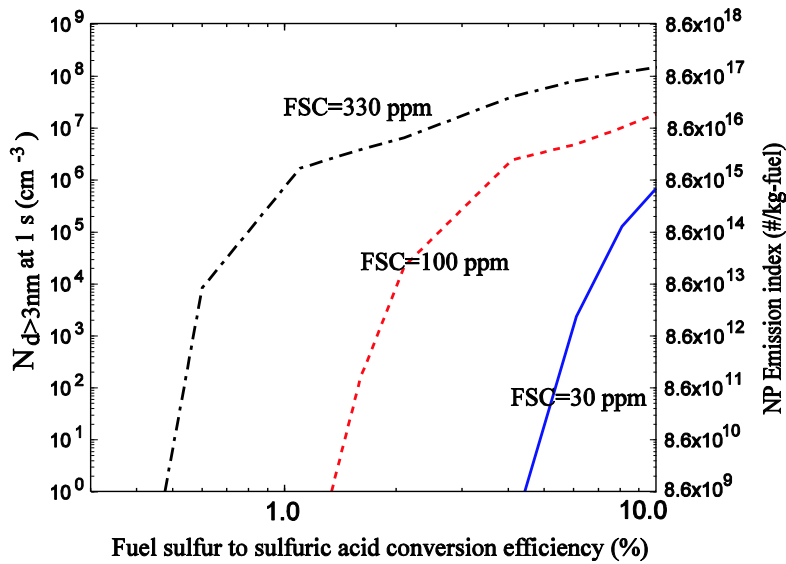


Figure 3.4. Effect of fuel sulfur conversion efficiency (ϵ_s) on $N_{d>3\text{ nm}}$ (at $t=1$ s) and NP emission index at three different FSCs (330 ppm, 100 ppm, 30 ppm). $N_{\text{soot}} = 10^7\text{ cm}^{-3}$. T_a and RH_a are 283 K and 60%, respectively.

Figure 3.4 illustrates $N_{d>3\text{ nm}}$ at plume age of 1 s as a function of ϵ_s . With a given FSC, the initial $[\text{H}_2\text{SO}_4]$ in the exhaust is proportional to ϵ_s . From Figure 3.4 we could see that $N_{d>3\text{ nm}}$ is very sensitive to ϵ_s , especially when ϵ_s is small. $N_{d>3\text{ nm}}$ increases by six orders of magnitude when ϵ_s increases from 1.5 % to 4.0 % for the case of 100 ppm of FSC. Thus, it is clear that ϵ_s is a critical parameter controlling NP production in engine exhaust. Since different vehicles have different catalytic converters, engine designs, and operation

conditions, it is reasonable to expect a wide range of ϵ_s for vehicles running on roadways. Obviously, more studies on ϵ_s for vehicles and the parameters affecting ϵ_s are needed. Since catalytic converters and other exhaust after-treatment devices may play an important role in oxidizing sulfur into sulfuric acid, future development of exhaust after-treatment devices should assess its sulfur oxidizing capacity because an increase in ϵ_s may significantly increase volatile NP emission (or the formation of volatile nucleation mode nanoparticles in engine exhaust).

3.4.4. Effects of Soot Scavenging

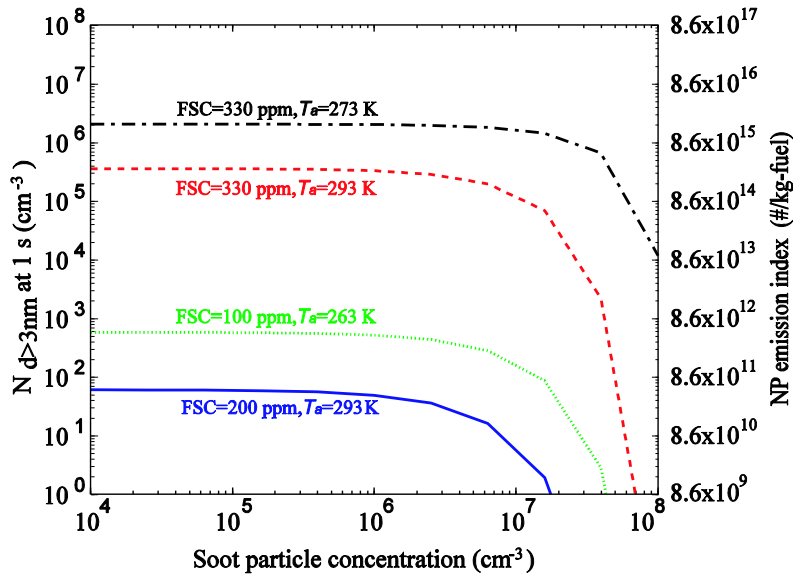


Figure 3.5. Effect of soot particle number concentration on $N_{d>3 \text{ nm}}$ (at $t=1 \text{ s}$) and NP emission index, at four different combinations of FSCs and T_a . The ambient relative humidity is 60% and $\epsilon_s = 1\%$.

Figure 3.5 gives $N_{d>3 \text{ nm}}$ as a function of soot concentrations. Soot scavenging effect is small when soot concentration is $< \sim 10^7 \text{ cm}^{-3}$ but is significant when soot concentration is $> \sim 10^7 \text{ cm}^{-3}$. Under the conditions investigated here, a reduction of soot particle concentration from 10^8 to 10^7 cm^{-3} increases the NP formation via homogeneous nucleation by up to five orders of magnitude. This is consistent with some measurements, which indicate that a reduction in soot concentration, as a result of cleaner modern engines or of using a particulate filter, actually leads to an increase in volatile NP emissions (Bagley et al., 1996; Graves, 1999). Nevertheless, our simulations suggest that the effect of soot emission reduction on volatile NP formation is limited after the soot concentration in the raw exhaust is reduced to below $\sim 10^7 \text{ cm}^{-3}$.

3.5. CONTRIBUTION OF ORGANIC SPECIES TO PARTICLE GROWTH IN ENGINE EXHAUST

Schemes to simulate the condensation of organic compounds on nanoparticles at earlier stages of plume dilution and evaporation of organic species from nanoparticles at later stages of plume dilution have been developed. The change in the volume concentration of organic components ($C_{i,org}$) in clusters/particles due to the condensation and evaporation of organic species is calculated using the following formulas:

$$\frac{\partial C_{i,org}}{\partial t} = \pi V_{org} f_{corr} n_i r_i^2 v_{org} (P_{org} - P_{s,org} A_{kelvin}) \quad (4)$$

$$f_{corr} = \frac{Kn_i}{0.75 + \zeta n_i} \quad (5)$$

$$A_{kelvin} = \exp\left(\frac{2\sigma_{rg} v_{rg}}{kT r_i}\right) \quad (6)$$

where V_{org} , v_{rg} , P_{org} , $P_{s,org}$, and σ_{rg} are the thermal speed, volume, vapor pressure, saturation vapor pressure, and surface tension of condensing organic species, respectively. f_{corr} is the correction factor accounting for the transition regime (J. H. Seinfeld and Pandis 1998), and Kn_i is the Knudsen number. A_{kelvin} accounts for the Kelvin effect, and r_i is the wet radius of clusters/particles in bin i .

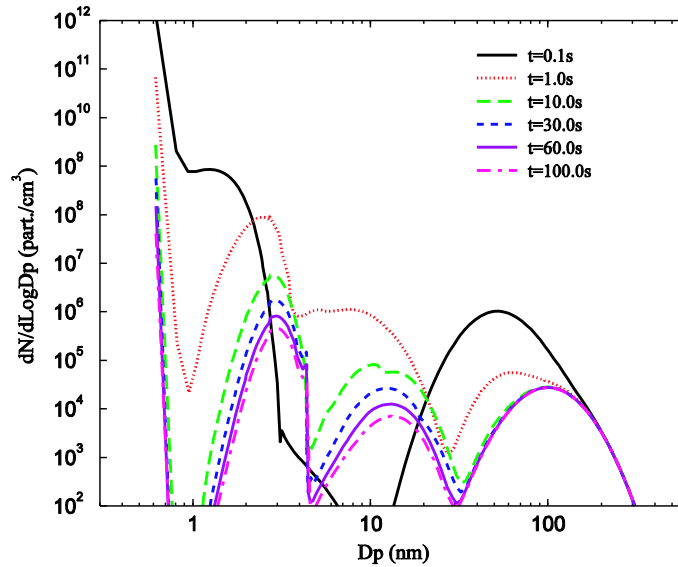


Figure 3.6. Number size distributions of NP formation and evolution on and near the roadway at six selected plume ages under high sulfur condition (FSC=330 ppm). The ambient temperature and relative humidity are assumed to be 278 K and 60 %, respectively. The size-distributions are not corrected with regard to dilution.

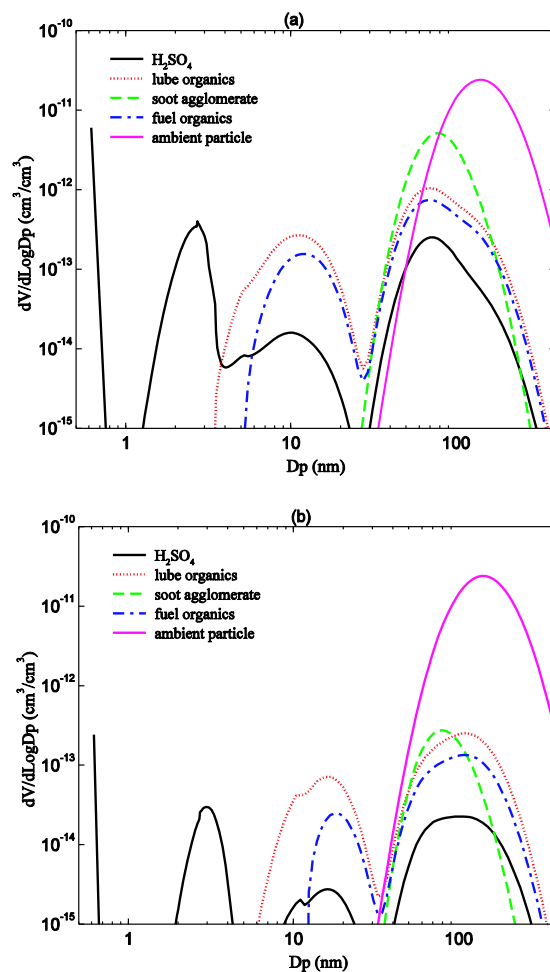


Figure 3.7. Simulated volume size distributions of H_2SO_4 , semi- and low volatile organics and soot in the particles at (a) $t=1$ s (a) and (b) $t=10$ s for the case shown in Figure 3.6.

Figure 3.6 shows the particle size distributions as a function of plume ages from 0 s to 100 s, and Figure 3.7 gives the compositions of particles as a function of particle sizes at two different plume ages ($t=1$ s and 10 s). Most of the nucleation happens within 0.2 s of plume age, and these nucleated particles continue to grow as a result of sulfuric acid condensation and self-coagulation. When the particles are big enough to overcome the Kelvin effect, both semi- and low volatile organics from fuel and lubricating oil further condense onto them and grow them to the sizes typically observed in the atmosphere. Our simulation shows that the time scale to form the nucleation mode is less than 1 s of plume age, which is consistent with the observations (Rönkkö et al., 2006) showing the development of the nucleation mode within ~ 0.45 s after the exhaust left the tailpipe. The geometrical mean sizes of the nucleation mode particles range from ~ 6 to ~ 20 nm, depending on the organic concentrations in the exhaust. The sulfuric acid vapor can grow the nucleated particles to around 3-4 nm but the organic compounds associated with unburned fuel and lubrication oils dominate the growth of these nucleated NPs to around 10-20 nm.

Before the plume reaches the roadside, semi-volatile organics already condensed on the NP may begin to evaporate due to the dilution (Figure 3.7). This immediate evaporation of semi-volatile organics upon emission has been suggested in other studies (Sakurai et al. 2003a,b; Jacobson et al. 2005; Robinson et al., 2007). Furthermore, our simulations show that as the plume is carried further away from roadway, both low and semi-volatile organics on the volatile NPs start to evaporate, causing the further shrinking of nucleation mode NPs.

Our study indicates that the mass in nucleation mode particles is dominated by the low and semi-volatile organics (Figure 3.7). The organics contribute to ~ 97 % of the mass of nucleation mode particles while sulfuric acid accounts for ~ 3 % of the total mass. For the accumulation mode, soot agglomerates dominate the mass. These predictions are generally consistent with the several volatilities studies of nucleation mode particles near the roadway (Sakurai et al. 2003; Kuhn et al. 2005a,b). Figure 3.7 also shows that most of the mass of H₂SO₄ and organics resides in the accumulation mode.

It is also important to notice that in addition to the typically observed nucleation mode with geometrical mean size of ~ 10 nm, our model predicts a second smaller yet high number concentration nucleation mode with the mean size of around 2 – 3 nm. The composition analysis shows that these small particles solely consist of H₂SO₄ and H₂O as a result of BHN. They are bigger than critical size and thus thermodynamically stable. However, without enough H₂SO₄ vapors, these particles are unable to grow large enough to overcome the Kelvin effect and be activated by organics. Due to their small sizes, they cannot be detected by current instruments. The coagulation kernel of those particles (~ 2 nm) with larger soot or ambient particles (~ 100 nm) is $\sim 3 \times 10^{-7} \text{ cm}^3/\text{s}$ at room temperature. Thus, their lifetime due to coagulation scavenge would be ~ 300 s, assuming ambient existing particle number concentration of 10^4 cm^{-3} . Thus, these particles may pose a negligible health threat to residents living hundreds of meters away from a roadway; however, they may be of concern to on-road commuters due to the much higher mobility and number concentration.

3.6 ROLE OF NON-VOLATILE CORES IN THE FORMATION OF NPS

If NPs are formed solely via BHN, the entire nucleation mode should be volatile, and will fully evaporate when heated. However, Sakurai et al. (2003) observed that 12 and 30 nm particles did not completely evaporate when heated up to 200 °C and the sizes of residual non-volatile cores were ~ 2-3 nm. Those residual particles were suggested to be composed of refractory materials such as metal oxide or non-volatile carbon species. Similar finding has been reported in other studies (Kuhn et al. 2005a; Biswas et al. 2007). In their dynamometer studies of diesel aerosol, Ntziachristos et al. (2004) found that small concentrations of sub-20 nm particles can be measured downstream of a thermo-denuder operating at 250 °C. Furthermore, Vaaraslahti et al. (2004) found that the observed nucleation mode at low engine loads (without after-

treatment) is independent of FSC. Kittelson et al. (2006a) observed non-volatile mode at idle condition and proposed that this non-volatile mode may be formed by nucleation of metallic species inside the engine.

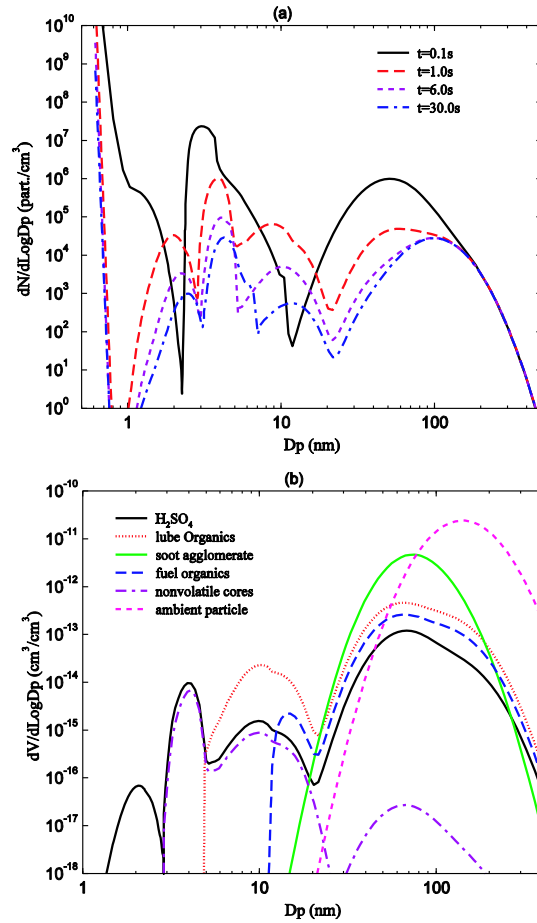


Figure 3.8. (a) Number size distributions of NPs at four selected plume ages, and (b) volume size distributions for different components at plume age of 1 s for the case with the presence of nanometer-sized solid cores. $T = 298\text{ K}$, $RH = 50\%$, $FSC = 50\text{ ppm}$, and $\varepsilon = 2.5\%$.

It appears that non-volatile nanometer-sized particles may contribute significantly to the observed NPs in vehicle exhausts under certain conditions. Following this thought, we simulated the NP formation and evolution with an assumed number concentration of refractory particles. The size range of refractory particles is assumed to be from 1.8 nm to 3 nm in diameter based on the study of Sakurai et al. (2003). The number concentration of the refractory particles is assumed to be 10^8 cm^{-3} . It should be noted that the actual size range and concentration of refractory particles are expected to depend strongly on engine operation condition, fuel and lube oil compositions, and soot concentration. In this simulation, ε_s is assumed to be 2.5 %. As one can see from Figure 3.8(a), in the presence of non-volatile nanometer-sized cores/particles in vehicular plumes, a clear nucleation mode with a mean size of $\sim 10\text{ nm}$ can be seen even with $FSC = 50$

ppm and $\kappa_s = 2.5$ (no such nucleation mode can form without the presence of the solid cores under the assumed conditions). Due to their large Kelvin effect, organics are not able to condense onto these small solid cores. However, sulfuric acid molecules, while not able to self-nucleate under the assumed condition, are able to condense on these solid cores. As some particles with non-volatile cores coated with H_2SO_4 grow big enough, they begin to uptake the semi- and low volatile organics and can grow to ~ 10 nm within one second. Figure 3.8(b) shows the compositions of particles of various sizes at 1 s of plume age. Organics still contribute to the majority of the mass in the nucleation mode particles. The volume fraction of refractory particles is comparable to that of H_2SO_4 and it accounts for less than 2 % of total mass of nucleation mode particles. This is consistent with the findings of Biswas et al. (2007), which showed that non-volatile fraction accounts for less than 3 % for 20 nm particles. The size and concentration of the nucleation mode particles depend on metal core size and concentration, the interaction between sulphuric acid and metal core mode, and the abundance of semi-volatile organics. While the refractory particles contribute negligibly to the nanoparticle mass, they are important to the formation of the NPs under the conditions when BHN is insufficient. Since metal additives have been widely used as the catalyst for diesel soot reduction and diesel particulate trap regeneration, more studies should be carried out to further investigate their role in NP formation.

4 REFERENCES

- Abdul-Khalek, I. S., D. B. Kittelson, and F. Brear, nanoparticle growth during dilution and cooling of diesel exhaust: Experimental investigation and theoretical assessment, *SAE Technical Paper Ser. No. 2000-01-0515*, 2000.
- Abdul-Khalek, I. S., D. B. Kittelson, and F. Brear, The influence of dilution conditions on diesel exhaust particle size distribution measurements, *SAE Technical Paper Ser. No. 1999-01-1142*, 1999.
- Bagley, S.T., K.J. Baumgard, L.G. Gratz, J.H. Johnson, and D.G. Leddy, Characterization of fuel and aftertreatment device effects on diesel emissions, *Health Effects Institute Res. Report No. 76*, 1996.
- Ball, S. M., D. R. Hanson, F. L. Eisele, P. H. McMurry, Laboratory studies of particle nucleation: Initial results for H₂SO₄, H₂O, and NH₃ vapors, *J. Geophys. Res.*, *104*, 23709-23718, 1999.
- Baumgard, K. J., and J. H. Johnson, The effect of fuel and engine design on diesel exhaust particle size distributions, *SAE Technical Paper Ser. No. 960131*, 1996.
- Biswas, S., L. Ntziachristos, et al., Particle volatility in the vicinity of a freeway with heavy-duty diesel traffic, *Atmospheric Environment*, *41*(16): 3479-3493, 2007.
- Donaldson, K., X.Y., Li, and W. MacNee, Ultrafine (nanometer) particle mediated lung injury, *J. Aerosol Sci.*, *29*, 553-560, 1998.
- Du, H. and F. Yu, Role of the binary H₂SO₄-H₂O homogeneous nucleation in the formation of volatile nanoparticles in the vehicular exhaust, *Atmospheric Environment*, *40*(39): 7579-7588, 2006.
- Gauderman, W. J., H. Vora, et al., Effect of exposure to traffic on lung development from 10 to 18 years of age: a cohort study, *Lancet* *369*(9561): 571-577, 2007.
- Graves, R. L., 1999. Review of diesel exhaust after treatment programs. SAE Technical Paper Series, No. 1999-01-2245.
- Jacobson, M. Z., D. B. Kittelson, et al., Enhanced coagulation due to evaporation and its effect on nanoparticle evolution, *Environmental Science and Technology* *39*(24): 9486-9492, 2005.
- Jung, H., D. B. Kittelson, et al., The influence of a cerium additive on ultrafine diesel particle emissions and kinetics of oxidation, *Combustion and Flame* *142*(3): 276-288, 2005.
- Kim, D., Gautam, M., Gera, D., Parametric studies of the formation of diesel particulate matter via nucleation and coagulation modes, *Journal of Aerosol Science*, *33*, 1609-1621, 2002.
- Kittelson, D. B., W. F. Watts and J. P. Johnson, Nanoparticle emissions on Minnesota highways, *Atmospheric Environment*, *38*, 9-19, 2004.
- Kittelson, D. B., W. F. Watts, et al., On-road and laboratory evaluation of combustion aerosols--Part I: Summary of diesel engine results, *Journal of Aerosol Science* *37*(8): 913-930, 2006a.
- Kittelson, D. B., W. F. Watts, et al., On-road evaluation of two diesel exhaust aftertreatment devices, *Journal of Aerosol Science* *37*(9): 1140-1151, 2006b.
- Kittelson, D.B., Engines and nanoparticles: a review, *J. Aerosol Sci.*, *29*, 575-588, 1998.
- Kittelson, D.B., Kadue, P.A., Scherrer, H.C., Loverien, R.E., Characterization of diesel particles in the atmosphere, *CRC, AP-2 Project Group*, 1988.

- Kittelson, D.B., Watts, W.F., Johnson, J.P., Gasoline vehicle exhaust particle sampling study. *DOE/NREL Final Report*, 2003.
- Kuhn, T., M. Krudysz, et al., Volatility of indoor and outdoor ultrafine particulate matter near a freeway, *Journal of Aerosol Science* 36(3): 291-302, 2005a.
- Kuhn, T., et al., Diurnal and seasonal characteristics of particle volatility and chemical composition in the vicinity of a light-duty vehicle freeway, *Atmospheric Environment* 39(37): 7154-7166, 2005b.
- Makar, P. A., The estimation of organic gas vapour pressure, *Atmos. Environ.*, 35, 961-974, 2001.
- Maricq, M.M., R.E. Chase, N. Xu and D.H. Podsiadlik, The effects of the catalytic converter and fuel sulfur level on motor vehicle particulate matter emissions gasoline vehicles, *Environmental Science and Technology*, 36, 276–282, 2002a.
- Maricq, M.M., R.E. Chase, N. Xu and P.M. Laing, The effects of the catalytic converter and fuel sulfur level on motor vehicle particulate matter emissions light duty diesel vehicles, *Environmental Science and Technology*, 36, 283–289, 2002b.
- Maynard, R. L., New Directions: Reducing the toxicity of vehicle exhaust, *Atmos. Environ.*, 34, 2667-2668, 2000.
- Meng, Y. Y., M. Wilhelm, et al., Traffic and outdoor air pollution levels near residences and poorly controlled asthma in adults, *Annals of Allergy, Asthma and Immunology* 98(5): 455-463, 2007.
- Nemmar, A., et al., Passage of Inhaled Particles Into the Blood Circulation in Humans, *Circulation*, 105, 411 – 414, 2002.
- Ntziachristos, L., et al., Performance evaluation of a novel sampling and measurement system for exhaust particle characterization, *Society of Automotive Engineer-Technical Papers 2004-01-1439*, 2004.
- Oberdörster, G., R. Gelein, J. Ferin, and B. Weiss, Association of particulate air pollution and acute mortality: involvement of ultrafine particles? *Inhalation Toxicology*, 7, 111-124, 1995.
- Peters, A., H. E. Wichmann, T. Tuch, J. Heinrich, and J. Heyder, Respiratory effects are associated with the number of ultrafine particles, *Am. J. Respir. Crit. Care Med.* 155, 1376-1383, 1997.
- Robinson, A.L., N.M. Donahue, M.K. Shrivastava, E.A. Weitkamp, A.M. Sage, A.P. Grieshop, T.E. Lane, J. R. Pierce, S.N. Pandis, Rethinking Organic Aerosols: Semivolatile Emissions and Photochemical Aging, *Science*, 315, 1259-1262, 2007.
- Rönkkö, T., et al., Effect of dilution conditions and driving parameters on nucleation mode particles in diesel exhaust: Laboratory and on-road study, *Atmospheric Environment* 40(16): 2893-2901, 2006.
- Rundell, K. W., J. R. Hoffman, et al., Inhalation of ultrafine and fine particulate matter disrupts systemic vascular function, *Inhalation Toxicology* 19(2): 133-140, 2007.
- Sakurai, H., H.J. Tobais, et al., On-line measurements of diesel nanoparticle composition, volatility, and hygroscopicity, *Atmospheric Environment*, 37, 1199–1210, 2003.
- Seaton, A., W. MacNee, K. Donaldson, and D. Godden, Particulate air pollution and acute health effects, *Lancet*, 345, 176-178, 1995.

- Shi, J. P., and R. M. Harrison, Investigation of ultrafine particle formation during diesel exhaust dilution, *Environ. Sci. Technol.*, 33, 3730-3736, 1999.
- Shi, J.P., R.M. Harrison, D.E. Evans, A. Alam, C. Barnes and G. Carter, A method for measuring particle number emissions from vehicles driving on the road, *Environmental Technology*, 23, 1–14, 2002.
- Tobias, H. J., et al., Chemical analysis of diesel engine nanoparticles using a nano-DMA/thermal desorption particle beam mass spectrometer, *Environ. Sci. Technol.*, 35, 2233-2243, 2001.
- Vaaraslahti, K., A. Virtanen, et al., Nucleation Mode Formation in Heavy-Duty Diesel Exhaust with and without a Particulate Filter, *Environ. Sci. Technol.* 38: 4884-4890, 2004.
- Vehkamäki H., M. Kulmala, I. Napari, K. E. J. Lehtinen, C. Timmreck, M. Noppel, and A. Laaksonen, An improved parameterization for sulfuric acid–water nucleation rates for tropospheric and stratospheric conditions, *J. Geophys. Res.*, 107 (D22), 4622, doi:10.1029/2002JD002184, 2002.
- Viisanen, Y., M. Kulmala, and A. Laaksonen, Experiments on gas-liquid nucleation of sulfuric acid and water, *J. Chem. Phys.*, 107, 920–926, 1997.
- Wichmann, H. E., et al., Daily mortality and fine and ultrafine particles in Erfurt, Germany, Part A: Role of particle number and particle mass, *HEI report*, 2000.
- Wold, L. E., B. Z. Simkhovich, et al., In vivo and in vitro models to test the hypothesis of particle-induced effects on cardiac function and arrhythmias, *Cardiovascular Toxicology* 6(1): 69-78, 2006.
- Yli-Tuomi, T., P. Aarnio, L. Pirjola, T. Mäkelä, R. Hillamo and M. Jantunen, Emissions of fine particles, NO_x, and CO from on-road vehicles in Finland, *Atmospheric Environment*, 39, 6696-6706, 2005.
- Yu, F., Quasi-unary homogeneous nucleation of H₂SO₄-H₂O. *J. Chem. Phys.*, 122, 074501, 2005.
- Yu, F., Binary H₂SO₄-H₂O homogeneous nucleation rates based on a kinetic quasi-unary model: Look-up tables, *Journal of Geophysical Research*, 111, D04201, doi:10.1029/2005JD006358, 2006.
- Yu, F., Chemiions and nanoparticle formation in diesel engine exhaust, *Geophys. Res. Lett.*, 28, 4191-4194, 2001.
- Yu, F., T. Lanni, and B. Frank, Measurements of ion concentration in gasoline and diesel engine exhaust, *Atmospheric Environment*, 38, 1417-1423, 2004.
- Zhang, K.M., A. S. Wexler, Y. F. Zhu, W. C. Hinds and C. Sioutas, Evolution of particle number distribution near roadways. Part II: the ‘Road-to-Ambient’ process, *Atmospheric Environment*, 38, 6655-6665, 2004.
- Zhang, K.M., and A. S. Wexler, Evolution of particle number distribution near roadways. Part I: analysis of aerosol dynamics and its implications for engine emission measurement. *Atmospheric Environment*, 38, 6643-6653, 2004.
- Zhu, Y., T. Kuhn, et al., Comparison of daytime and nighttime concentration profiles and size distributions of ultrafine particles near a major highway, *Environ. Sci. and Tech.* 40(8): 2531-2536, 2006.
- Zhu, Y., W.C. Hinds, S. Kim and C. Sioutas, Concentration and size distribution of ultrafine particles near a major highway, *Journal of the Air and Waste Management Association*, 52, 1032–1042, 2002a.

Zhu, Y., W.C. Hinds, S. Kim, S. Shen and C. Sioutas, Seasonal trends of concentration and size distribution of ultrafine particles near major highways in Los Angeles, *Aerosol Science and Tech.*, 38, 5–13, 2004.

Zhu, Y., W.C. Hinds, S. Kim, S. Shen and C. Sioutas, Study of ultrafine particles near a major highway with heavy-duty diesel traffic, *Atmospheric Environment*, 36, 4323–4335, 2002b.

For information on other
NYSERDA reports, contact:

New York State Energy Research
and Development Authority
17 Columbia Circle
Albany, New York 12203-6399

toll free: 1 (866) NYSERDA
local: (518) 862-1090
fax: (518) 862-1091

info@nysesda.org
www.nysesda.org

FORMATION OF VOLATILE NANOPARTICLES IN MOTOR VEHICLE EXHAUST

FINAL REPORT 07-12

STATE OF NEW YORK
ELIOT SPITZER, GOVERNOR

NEW YORK STATE ENERGY RESEARCH AND DEVELOPMENT AUTHORITY
VINCENT A. DEIORIO, ESQ., CHAIRMAN
PETER R. SMITH, PRESIDENT, AND CHIEF EXECUTIVE OFFICER

